

GenMol: A Drug Discovery Generalist with Discrete Diffusion

Seul Lee^{2*}, Karsten Kreis¹, Srimukh Prasad Veccham¹, Meng Liu¹, Danny Reidenbach¹, Yuxing Peng¹, Saeed Paliwal¹, Weili Nie^{1†}, Arash Vahdat^{1†}

¹ NVIDIA ² KAIST

Abstract: Drug discovery is a complex process that involves multiple scenarios and stages, such as fragment-constrained molecule generation, hit generation and lead optimization. However, existing molecular generative models can only tackle one or two of these scenarios and lack the flexibility to address various aspects of the drug discovery pipeline. In this paper, we present *Generalist Molecular generative model* (GenMol), a versatile framework that addresses these limitations by applying discrete diffusion to the Sequential Attachment-based Fragment Embedding (SAFE) molecular representation. GenMol generates SAFE sequences through non-autoregressive bidirectional parallel decoding, thereby allowing utilization of a molecular context that does not rely on the specific token ordering and enhanced computational efficiency. Moreover, under the discrete diffusion framework, we introduce *fragment remasking*, a strategy that optimizes molecules by replacing fragments with masked tokens and regenerating them, enabling effective exploration of chemical space. GenMol significantly outperforms the previous GPT-based model trained on SAFE representations in *de novo* generation and fragment-constrained generation, and achieves state-of-the-art performance in goal-directed hit generation and lead optimization. These experimental results demonstrate that GenMol can tackle a wide range of drug discovery tasks, providing a unified and versatile approach for molecular design.

1. Introduction

Discovering molecules with the desired chemical profile is the core objective of drug discovery (Hughes et al., 2011). To achieve the ultimate goal of overcoming disease, a variety of drug discovery approaches have been established. For example, fragment-constrained molecule generation is a popular strategy for designing new drug candidates under the constraint of preserving a certain molecular substructure already known to exhibit a particular bioactivity (Murray & Rees, 2009). Furthermore, real-world drug discovery pipelines are not a single stage but consist of several key stages, such as hit generation and lead optimization (Hughes et al., 2011). A drug discovery process that leads to the finding of successful drug candidates that can enter clinical trials should consider all of these different scenarios.

Generative models have emerged as a promising methodology to greatly accelerate labor-intensive drug discovery pipelines (Olivecrona et al., 2017; Jin et al., 2018; Yang et al., 2021; Lee et al., 2023), but previous molecular generative models have a common limitation: they focus on only one or two of the drug discovery scenarios. They either cannot be applied to multiple tasks or require expensive modifications including retraining of a specific architecture for each task (Yang et al., 2020; Guo et al., 2023). Recently, SAFE-GPT (Noutahi et al., 2024) has been proposed to address this problem by using Sequential Attachment-based Fragment Embedding (SAFE) that represents a molecule as an unordered

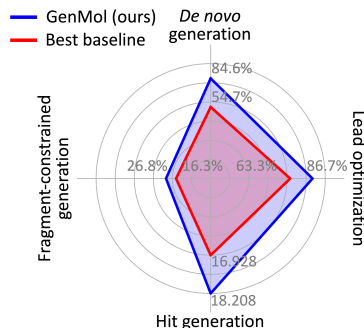


Figure 1 | Results on various drug discovery tasks. The values are quality, average quality, sum AUC top-10, and success rate for *de novo* generation, fragment-constrained generation, hit generation, and lead optimization, respectively. The “best baseline” refers to multiple best-performing task-specific models among prior works.

sequence of Simplified Molecular Input Line Entry System (SMILES) (Weininger, 1988) fragment blocks and viewing fragment-constrained generation as a sequence completion task. However, since all sequence-based molecular representations including SMILES and SAFE have an ordering of tokens based on heuristic rules such as depth-first search (DFS), autoregressive models that operate in a left-to-right order like GPT are unnatural for processing and generating molecular sequences. In addition, the autoregressive decoding scheme limits the computational efficiency of the model. Moreover, SAFE-GPT relies on fine-tuning under expensive reinforcement learning (RL) objectives to be applied to goal-directed molecule generation (Noutahi et al., 2024).

* Work done during an internship at NVIDIA. [†] Equal advising.
© 2025 NVIDIA. All rights reserved.

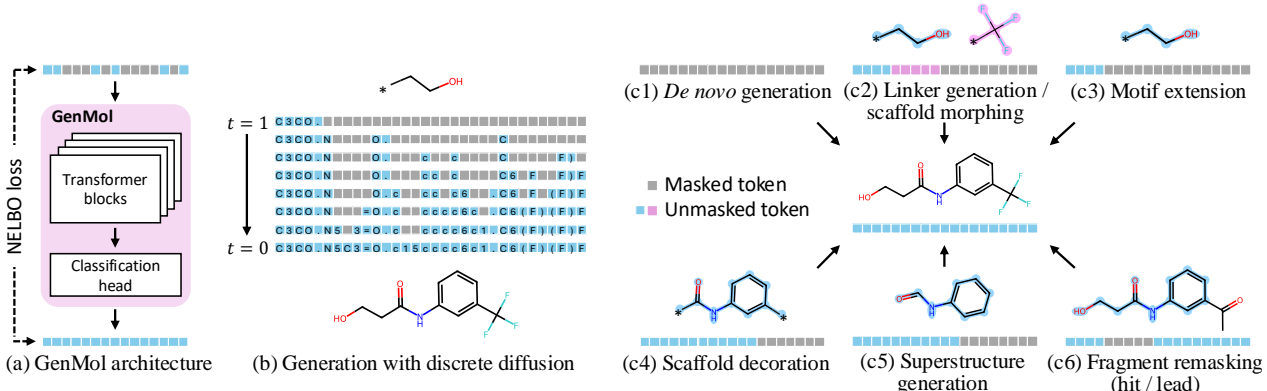


Figure 2 | (a) GenMol architecture. GenMol adopts the BERT architecture and is trained with the NELBO loss of masked discrete diffusion. **(b) Generation process of GenMol.** Under masked discrete diffusion, GenMol completes a molecule by simulating backward in time and predicting masked tokens at each time step t until all tokens are unmasked. **(c) Illustration of various drug discovery tasks that can be performed by GenMol.** GenMol is endowed with the ability to easily perform (c1) *de novo* generation, (c2-c5) fragment-constrained generation, and (c6) fragment remasking that can be applied to goal-directed hit generation and lead optimization.

To this end, we propose *Generalist Molecular generative model* (GenMol), a versatile molecular generation framework that is endowed with the ability to handle diverse scenarios that can be encountered in the multifaceted drug discovery pipeline (Figure 2). Specifically, GenMol adopts a masked discrete diffusion framework (Austin et al., 2021; Sahoo et al., 2024) with the BERT architecture (Devlin et al., 2019) to generate SAFE molecular sequences, thereby enjoying several advantages. Discrete diffusion allows GenMol to exploit a molecular context that does not rely on the specific ordering of tokens and fragments by bidirectional attention. Additionally, the non-autoregressive parallel decoding improves GenMol’s computational efficiency without degrading the generation quality (Figure 2(b)). Furthermore, discrete diffusion enables GenMol to explore chemical space with a simple yet effective remasking strategy. Concretely, we propose *fragment remasking* (Figure 2(c6) and Figure 3), a strategy to optimize molecules by replacing certain fragments in a given molecule with masked tokens, from which discrete diffusion generates new fragments. By utilizing fragments as the explorative unit instead of individual tokens, GenMol can effectively and efficiently explore the vast chemical space to find chemical optima.

We experimentally validate GenMol on a wide range of molecule generation tasks that simulate real-world drug discovery problems, including *de novo* generation, fragment-constrained generation, goal-directed hit generation, and goal-directed lead optimization. Across extensive experiments, GenMol outperforms existing methods by a large margin (Figure 1). Note that the best baseline results shown in Figure 1 are not the results of a single model, but of multiple task-specific models. These results demon-

strate GenMol's potential as a versatile tool that can be used throughout the drug discovery pipeline.

We summarize our contributions as follows:

- We introduce GenMol, a framework for unified and versatile molecule generation through applying discrete diffusion to the SAFE representation.
- We propose fragment remasking, an effective strategy for exploring chemical space using molecular fragments as the unit of exploration.
- We validate the efficacy and versatility of GenMol on a wide range of drug discovery tasks.

2. Related Work

Discrete diffusion. There has been steady progress in applying discrete diffusion for discrete data generation, especially in NLP tasks (Hoogeboom et al., 2021; Austin et al., 2021; He et al., 2023; Zheng et al., 2024; Lou et al., 2024; Sahoo et al., 2024). This is mainly due to their non-autoregressive generation property, which leads to a potential for better modeling long-range dependencies and accelerating sampling speed, and their flexible design choices in training, sampling, and controllable generation (Sahoo et al., 2024). Notably, D3PM (Austin et al., 2021) introduced a general framework with a Markov forward process represented by transition matrices, and a transition matrix with an absorbing state corresponds to the masked language modeling (MLM) such as BERT (Devlin et al., 2019). Campbell et al. (2022) proposed a continuous-time framework for discrete diffusion models based on the continuous-time Markov chain (CTMC) theory. SEDD (Lou et al., 2024) introduced a denoising score entropy loss that extends score matching to discrete diffusion models.

Sahoo et al. (2024) and Shi et al. (2024) proposed simple masked discrete diffusion frameworks, with the training objective being a weighted average of MLM losses across different diffusion time steps.

Recently, a few works have applied discrete diffusion for molecular generation. For instance, DiGress (Vignac et al., 2023) followed the D3PM framework to generate molecular graphs with categorical node and edge attributes. Other works (Zhang et al., 2023; Lin et al., 2024; Hua et al., 2024) focused on the 3D molecular structure generation, where they used discrete diffusion for atom type generation and continuous diffusion for atom position generation. However, none of them applied discrete diffusion for molecular sequence generation that can serve as a generalist foundation model for solving various downstream tasks.

Fragment-based drug discovery. Fragment-based molecular generative models refer to a class of methods that reassemble existing molecular substructures (i.e., fragments) to generate new molecules. A line of works (Jin et al., 2020; Maziarz et al., 2021; Kong et al., 2022; Geng et al., 2023) used graph-based VAEs to generate novel molecules conditioned on discovered substructures. Besides, Xie et al. (2020) proposed to progressively add or delete fragments of molecular graphs using Markov chain Monte Carlo (MCMC) sampling. Yang et al. (2021) proposed a reinforcement learning (RL) framework with prioritized experience replay to assemble fragments.

Graph-based genetic algorithms (GAs) (Jensen, 2019; Tripp & Hernández-Lobato, 2023) remain as a strong approach, which decompose parent molecules into fragments that are combined to generate an offspring molecule. Since their fragment-based strategies are limited by the fact that their generation is from random combinations of existing fragments with a local mutation of a small probability, they suffer from limited exploration in the chemical space. More recently, *f*-RAG (Lee et al., 2024a) introduced a fragment-level retrieval framework that augments the pre-trained molecular language model SAFEGPT (Noutahi et al., 2024), where retrieving fragments from dynamically updated fragment vocabulary largely improves the exploration-exploitation trade-off. However, *f*-RAG (Lee et al., 2024a) still needs to train an information fusion module before adapting to various goal-oriented generation tasks.

3. Background

3.1. Masked Diffusion

Among various discrete diffusion frameworks, we follow MDLM (Sahoo et al., 2024) to define our masked

diffusion model, due to its simplicity and effectiveness.

Formally, we define \mathbf{x} as a sequence of L discrete tokens, each of which, denoted as \mathbf{x}^l , is a one-hot vector with K categories (i.e., $\mathbf{x}_i^l \in \{0, 1\}^K$ and $\sum_{i=1}^K \mathbf{x}_i^l = 1$). Without loss of generality, we assume the K -th category represents the masking token, whose one-hot vector is denoted by \mathbf{m} (i.e., $\mathbf{m}_K = 1$). We also define $\text{Cat}(\cdot; \boldsymbol{\pi})$ as a categorical distribution with a probability $\boldsymbol{\pi} \in \Delta^K$, where Δ^K represents the simplex over K categories.

The forward masking process in the masked diffusion independently interpolates between each token in clean data sequence \mathbf{x}^l and the masking token \mathbf{m} , which is defined as

$$q(\mathbf{z}_t^l | \mathbf{x}^l) = \text{Cat}(\mathbf{z}_t^l; \alpha_t \mathbf{x}^l + (1 - \alpha_t) \mathbf{m}), \quad (1)$$

where \mathbf{z}_t^l denotes the l -th token in the noisy data sequence at the time step $t \in [0, 1]$, and $\alpha_t \in [0, 1]$ denotes the masking ratio that is monotonically decreasing function of t , with $\alpha_0 = 1$ to $\alpha_1 = 0$. Accordingly, at time step $t = 1$, \mathbf{z}_t becomes a sequence of all masked tokens.

The reverse unmasking process inverts the masking process and independently infers each token of the less masked data \mathbf{z}_s from more masked data \mathbf{z}_t with $s < t$, which is given by

$$p_\theta(\mathbf{z}_s^l | \mathbf{z}_t^l) = \begin{cases} \text{Cat}(\mathbf{z}_s^l; \mathbf{z}_t^l), & \mathbf{z}_t^l \neq \mathbf{m}, \\ \text{Cat}(\mathbf{z}_s^l; \frac{(1-\alpha_s)\mathbf{m} + (\alpha_s - \alpha_t)\mathbf{x}_\theta^l(\mathbf{z}_t, t)}{1-\alpha_t}), & \mathbf{z}_t^l = \mathbf{m}, \end{cases} \quad (2)$$

where $\text{Cat}(\mathbf{x}; \boldsymbol{p})$ is a categorical distribution over the vector \mathbf{x} with probabilities given by the vector \boldsymbol{p} and $\mathbf{x}_\theta(\mathbf{z}_t, t)$ is a denoising network that takes the full L tokens in the noisy data sequence \mathbf{z}_t as input and predicts L probability vectors for the clean data sequence. This parameterization designs the reverse process such that it does not change unmasked tokens. To train the denoising network $\mathbf{x}_\theta(\mathbf{z}_t, t)$, the training objective, which implicitly approximates the negative ELBO (Sohl-Dickstein et al., 2015), is given by

$$\mathcal{L}_{\text{NELBO}} = \mathbb{E}_q \int_0^1 \frac{\alpha'_t}{1 - \alpha_t} \sum_l \log \langle \mathbf{x}_\theta^l(\mathbf{z}_t, t), \mathbf{x}^l \rangle dt, \quad (3)$$

which is the weighted average of MLM losses (i.e., cross-entropy losses) over time steps.

3.2. SAFE Molecular Representation

Simplified Molecular Input Line Entry System (SMILES) (Weininger, 1988) is the most widely used molecular string representation, but it relies on a heuristic depth-first search (DFS) that traverses the atoms of a molecule. Therefore, atoms that are

close in molecular structure can be tokens that are very far apart in molecular sequence, and thus it is not straightforward to perform fragment-constrained molecular generation with SMILES.

Sequential Attachment-based Fragment Embedding (SAFE) (Noutahi et al., 2024) has recently been proposed to alleviate this problem. SAFE represents molecules as an unordered sequence of fragment blocks, thereby casting molecular design tasks into sequence completion tasks. SAFE is a non-canonical SMILES that restricts the arrangement of SMILES tokens corresponding to the same molecular fragment to be consecutive. Molecules are decomposed into fragments by the BRICS algorithm (Degen et al., 2008) and the fragments are concatenated using a dot token (“.”) while preserving their attachment points. SAFE is permutation-invariant on fragments, i.e., the order of fragments within a SAFE string does not change the molecular identity.

4. Method

Now we introduce GenMol, a universal molecule generation framework that can solve various drug discovery tasks. We first introduce the construction of the discrete diffusion framework on the SAFE representation in Section 4.1. Next, we describe fragment remasking, an effective exploration strategy of GenMol for goal-oriented generation tasks, in Section 4.2.

4.1. Masked Diffusion for Molecule Generation

We apply discrete diffusion to the SAFE molecular representation to establish a flexible and efficient molecule generation framework. Specifically, GenMol adopts the architecture of BERT (Devlin et al., 2019) as the denoising network \mathbf{x}_θ and the training scheme of MDLM described in Section 3.1. Utilizing a discrete diffusion framework instead of an autoregressive model is more in line with the SAFE molecular representation and has several advantages. First, due to the bidirectional attention mechanism in BERT, GenMol can leverage parallel decoding where all tokens are decoded simultaneously under discrete diffusion (Figure 5). As SAFE sequences are fragment order-insensitive, this allows GenMol to predict masked tokens with a better inductive bias by looking backward and forward in the sequence. The non-autoregressive parallel decoding scheme also improves GenMol’s efficiency without degrading its generation quality. Furthermore, the discrete diffusion framework enables GenMol to explore the neighborhood of a given molecule in chemical space with a simple yet effective remasking strategy, which will be described in detail in Section 4.2.

During inference, inspired by Chang et al. (2022) and Tang et al. (2022), GenMol employs *confidence sampling*, a strategy that decides which tokens to unmask at each sampling step based on the confidence scores of the tokens. At each masked index l , GenMol samples a token \mathbf{z}_s^l based on the reverse unmasking process $p_\theta(\mathbf{z}_s^l | \mathbf{z}_t)$ calculated by $\mathbf{x}_\theta^l(\mathbf{z}_t, t)$. Here, we introduce the softmax temperature τ to the logits of $\mathbf{x}_\theta^l(\mathbf{z}_t, t)$ as follows:

$$p_{\theta,i}^l = \frac{\exp(\log \mathbf{x}_{\theta,i}^l(\mathbf{z}_t^l, t) / \tau)}{\sum_{i=1}^K \exp(\log \mathbf{x}_{\theta,i}^l(\mathbf{z}_t^l, t) / \tau)} \text{ for } i = 1, \dots, K. \quad (4)$$

After sampling from the probability specified by Eq. (4), the corresponding prediction score p_{θ,i^*}^l is used as the confidence score of \mathbf{z}_s^l , where i^* is the index of the sampled token. We further introduce a gumbel noise decreasing over the sampling process, yielding the final confidence score of \mathbf{z}_s^l as follows:

$$\log p_{\theta,i^*}^l + r \cdot t \cdot \epsilon, \quad \epsilon \sim \text{Gumbel}(0, 1), \quad (5)$$

where r is the randomness and t is the current time step. Trade-offs between molecular quality and diversity often arise in drug discovery problems, and GenMol is able to balance these two essential considerations through the softmax temperature τ and the randomness r , as we will show in Section 5.1.

The number of tokens N to unmask at each time step is defined by the mask schedule, and GenMol unmask the top- N currently masked tokens based on their confidence scores (Eq. (5)). In other words, this is equivalent to predicting all tokens simultaneously, but only confirming the most confident predictions. The other tokens are masked again and predicted in the next step. With confidence sampling, GenMol can exploit the dependencies between tokens in a given molecular sequence for better sampling quality, rather than randomly and independently selecting tokens to unmask, as in the standard diffusion sampling (Austin et al., 2021; Sahoo et al., 2024).

4.2. Exploration with Fragment Remasking

Under the discrete diffusion framework of GenMol, we propose *fragment remasking* (Figure 3), an effective strategy to explore the neighborhood of a given molecule in chemical space and find optimized molecules. Discrete diffusion allows GenMol to mask and re-predict some tokens of a given molecule, making neighborhood exploration simple and straightforward. However, although there exist some works that apply token-wise remasking to protein sequence optimization (Hayes et al., 2024; Gruver et al., 2024), it would be suboptimal to naively adopt the same

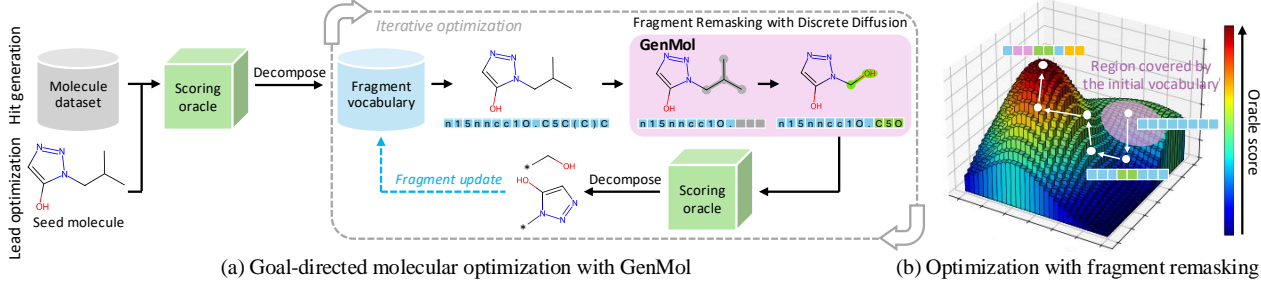


Figure 3 | (a) **Goal-directed hit generation and lead optimization process with GenMol.** An initial fragment vocabulary is constructed by decomposing an existing molecule dataset (hit generation) or a seed molecule (lead optimization), two fragments are randomly sampled from the vocabulary and connected to provide a starting molecule to GenMol. GenMol performs fragment remasking, a strategy to modify molecules by randomly selecting a fragment in a given molecule and replacing it with a mask chunk, and then generating a new fragment. The fragment vocabulary is updated with the generated molecules for the next iteration. (b) **Illustration of the molecular optimization trajectory with fragment remasking.** With discrete diffusion-based fragment remasking, GenMol can explore beyond the initial fragment vocabulary to find chemical optima.

strategy for small molecule optimization. This is because each token in a SAFE (or SMILES) sequence represents a single atom or bond, and masking them individually results in localized and ineffective exploration. The structure and activity of molecules are highly correlated, which is known as the structure-activity relationship (SAR) (Bohacek et al., 1996), and the units that carry information about molecular properties are fragments, not individual atoms or bonds. Inspired by the principle of SAR, fragment remasking modifies molecules by randomly selecting a fragment in a given molecule and replacing it with a fragment mask chunk, from which discrete diffusion generates a new molecular fragment. The proposed fragment remasking can also be viewed as a mutation operation in GA where the mutation is performed at the fragment-level rather than at the atom- or bond-level. We will examine the superiority of fragment remasking over token remasking in Section 5.5.

The lengths of the fragment mask chunks are sampled from a predefined distribution, e.g., the distribution of fragment lengths in the training molecule. The length of the fragment depends on the decomposition rule used, and instead of using a fixed length, this strategy allows GenMol to automatically adjust the length based on the decomposition rule. This also ensures that GenMol generates fragments of varying lengths, offering users better controllability over molecule generation.

5. Experiments

GenMol is trained on the SAFE dataset (Noutahi et al., 2024), which combines molecules from ZINC (Irwin & Shoichet, 2005) and UniChem (Chambers et al., 2013). With this single trained model, we demonstrate that GenMol can be universally and effectively applied to a wide range of molecule generation tasks

simulating various real-world drug discovery scenarios. We emphasize that a single GenMol checkpoint is used to perform the following tasks without any additional finetuning specific to each task. We first conduct experiments on a *de novo* molecule generation task in Section 5.1. Next, we conduct experiments on fragment-constrained molecule generation tasks in Section 5.2. We then examine GenMol’s ability to perform goal-directed hit generation and goal-directed lead optimization in Section 5.3 and Section 5.4, respectively. We perform ablation studies in Section 5.5.

5.1. De Novo Generation

Setup. In *de novo* generation, the goal is to generate valid, unique, and diverse molecules. We generate 1,000 molecules and evaluate them with the following metrics, following Noutahi et al. (2024). **Validity** is the fraction of generated molecules that are chemically valid. **Uniqueness** is the fraction of valid molecules that are unique. **Diversity** is defined as the average pairwise Tanimoto distance between the Morgan fingerprints of the generated molecules. We further introduce **quality**, the fraction of generated molecules that are valid, unique, drug-like, and synthesizable, to provide a single metric that summarizes validity and uniqueness and evaluates the model’s ability to generate chemically reasonable molecules. Here, *drug-like* and *synthesizable* molecules are defined as those satisfying quantitative estimate of drug-likeness (QED) (Bickerton et al., 2012) ≥ 0.6 and synthetic accessibility (SA) (Ertl & Schuffenhauer, 2009) ≤ 4 , respectively, following Jin et al. (2020). Further details are provided in Section A.3.

Results. The results of *de novo* generation are shown in Table 1. Both GenMol and SAFE-GPT (Noutahi et al., 2024) show near-perfect unique-

Table 1 | ***De novo* molecule generation results.** The results are the means and the standard deviations of 3 runs. N , τ , and r is the number of tokens to unmask at each time step, the softmax temperature, and the randomness, respectively. The best results are highlighted in bold.

Method	Validity (%)	Uniqueness (%)	Quality (%)	Diversity	Sampling time (s)
SAFE-GPT	94.0 ± 0.4	100.0 ± 0.0	54.7 ± 0.3	0.879 ± 0.001	27.7 ± 0.1
GenMol ($\tau = 0.5, r = 0.5$)					
$N = 1$	100.0 ± 0.0	99.7 ± 0.1	84.6 ± 0.8	0.818 ± 0.001	21.1 ± 0.4
$N = 2$	97.6 ± 0.7	99.5 ± 0.2	76.2 ± 1.3	0.843 ± 0.002	12.2 ± 0.6
$N = 3$	95.6 ± 0.5	99.0 ± 0.1	67.1 ± 0.7	0.861 ± 0.001	10.1 ± 0.2
GenMol ($N = 1$)					
$\tau = 0.5, r = 0.5$	100.0 ± 0.0	99.7 ± 0.1	84.6 ± 0.8	0.818 ± 0.001	21.1 ± 0.4
$\tau = 0.5, r = 1.0$	99.7 ± 0.1	100.0 ± 0.0	83.8 ± 0.5	0.832 ± 0.001	20.5 ± 0.6
$\tau = 0.5, r = 10.0$	99.6 ± 0.1	99.9 ± 0.0	75.0 ± 0.6	0.858 ± 0.002	21.6 ± 0.4
$\tau = 1.0, r = 10.0$	99.8 ± 0.1	99.6 ± 0.1	63.0 ± 0.4	0.882 ± 0.003	21.5 ± 0.5
$\tau = 1.5, r = 10.0$	95.6 ± 0.3	98.3 ± 0.2	39.7 ± 0.5	0.911 ± 0.004	20.9 ± 0.5

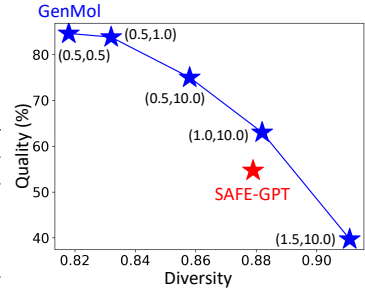


Figure 4 | **The quality-diversity trade-off in *de novo* generation** with different values of (τ, r) .

Table 2 | **Fragment-constrained molecule generation results.** The results are the means and the standard deviations of 3 runs. The best results are highlighted in bold.

Method	Task	Validity (%)	Uniqueness (%)	Quality (%)	Diversity	Distance
SAFE-GPT	Linker design	76.6 ± 5.1	82.5 ± 1.9	21.7 ± 1.1	0.545 ± 0.007	0.541 ± 0.006
	Scaffold morphing	58.9 ± 6.8	70.4 ± 5.7	16.7 ± 2.3	0.514 ± 0.011	0.528 ± 0.009
	Motif extension	96.1 ± 1.9	66.8 ± 1.2	18.6 ± 2.1	0.562 ± 0.003	0.665 ± 0.006
	Scaffold decoration	97.7 ± 0.3	74.7 ± 2.5	10.0 ± 1.4	0.575 ± 0.008	0.625 ± 0.009
	Superstructure generation	95.7 ± 2.0	83.0 ± 5.9	14.3 ± 3.7	0.573 ± 0.028	0.776 ± 0.036
GenMol	Linker design	100.0 ± 0.0	83.7 ± 0.5	21.9 ± 0.4	0.547 ± 0.002	0.563 ± 0.003
	Scaffold morphing	100.0 ± 0.0	83.7 ± 0.5	21.9 ± 0.4	0.547 ± 0.002	0.563 ± 0.003
	Motif extension	77.2 ± 0.1	77.8 ± 0.2	27.5 ± 0.8	0.617 ± 0.002	0.682 ± 0.002
	Scaffold decoration	96.8 ± 0.2	78.0 ± 1.2	29.6 ± 0.8	0.576 ± 0.001	0.650 ± 0.001
	Superstructure generation	98.2 ± 1.1	78.3 ± 3.4	33.3 ± 1.6	0.574 ± 0.008	0.757 ± 0.003

ness, while GenMol significantly outperforms SAFE-GPT in terms of validity, quality, and sampling time. Thanks to the non-autoregressive parallel decoding scheme, GenMol can predict multiple tokens simultaneously and shows much faster sampling as N , the number of tokens to unmask at each time step, increases. Notably, GenMol with $N = 3$ shows higher quality than SAFE-GPT with 2.7x shorter sampling time and similar diversity. Furthermore, GenMol has the ability to balance between quality and diversity by adjusting the values of the softmax temperature τ and the randomness r of the confidence sampling described in Section 4.1. This balance is also shown in Figure 4, demonstrating that GenMol generates molecules along the Pareto frontier of the quality-diversity trade-off. Further analysis on quality and diversity are provided in Section B.1 and Section B.2.

5.2. Fragment-constrained Generation

Setup. In fragment-constrained generation, the goal is to complete molecules given a set of fragments, a frequently encountered setting in real-world drug discovery scenarios. We use the benchmark proposed by Noutahi et al. (2024), which uses input fragments extracted from 10 known drugs to perform the **linker design**, **scaffold morphing**, **motif extension**, **scaffold decoration**, and **superstructure generation** tasks. In addition to **validity**, **uniqueness**, **diver-**

sity, and **quality** introduced in Section 5.1, **distance**, the average Tanimoto distance between the generated molecules and the original molecules, is also measured. 100 molecules are generated for each drug and averaged to calculate the metrics. Further details are provided in Section A.4.

Results. The results of fragment-constrained generation are shown in Table 2. GenMol significantly outperforms SAFE-GPT on most metrics across the tasks, demonstrating its general applicability to a variety of fragment constraint generation settings. Especially, GenMol is superior to SAFE-GPT in generating high-quality molecules while preserving high diversity under the fragment constraints, again validating the superiority of GenMol in balancing between quality and diversity.

5.3. Goal-directed Hit Generation

Setup. In goal-directed hit generation, the goal is to generate hits, i.e., molecules that are optimized in terms of target chemical properties. Following Lee et al. (2024b) and Lee et al. (2024a), we first construct a fragment vocabulary by fragmenting the molecules in the ZINC250k dataset (Irwin et al., 2012). During generation, a molecule is generated by randomly selecting two fragments from the vocabulary and concatenating them, and then applying the fragment

Table 3 | Goal-directed hit generation results. The results are the means of PMO AUC top-10 of 3 runs. The results for *f*-RAG (Lee et al., 2024a), Genetic GFN (Kim et al., 2024) and Mol GA (Tripp & Hernández-Lobato, 2023) are taken from the respective papers and the results for REINVENT and Graph GA are taken from Gao et al. (2022). The best results are highlighted in bold.

Oracle	GenMol	GenMol-TR	GenMol-NR	<i>f</i> -RAG	Genetic GFN	Mol GA	REINVENT	Graph GA
albuterol_similarity	0.932	0.895	0.872	0.977	0.949	0.896	0.882	0.838
amlodipine_mpo	0.804	0.802	0.769	0.749	0.761	0.688	0.635	0.661
celecoxib_rediscovery	0.826	0.821	0.859	0.778	0.802	0.567	0.713	0.630
deco_hop	0.953	0.945	0.917	0.936	0.733	0.649	0.666	0.619
drd2	0.995	0.995	0.995	0.992	0.974	0.936	0.945	0.964
felofenadine_mpo	0.894	0.886	0.875	0.856	0.856	0.825	0.784	0.760
gsk3b	0.986	0.985	0.985	0.969	0.881	0.843	0.865	0.788
isomers_c7h8n2o2	0.934	0.934	0.897	0.955	0.969	0.878	0.852	0.862
isomers_c9h10n2o2pf2cl	0.833	0.830	0.816	0.850	0.897	0.865	0.642	0.719
jnk3	0.856	0.848	0.845	0.904	0.764	0.702	0.783	0.553
median1	0.397	0.397	0.397	0.340	0.379	0.257	0.356	0.294
median2	0.355	0.350	0.349	0.323	0.294	0.301	0.276	0.273
mestranol_similarity	0.981	0.980	0.970	0.671	0.708	0.591	0.618	0.579
osimertinib_mpo	0.876	0.876	0.876	0.866	0.860	0.844	0.837	0.831
perindopril_mpo	0.703	0.703	0.697	0.681	0.595	0.547	0.537	0.538
qed	0.942	0.942	0.927	0.939	0.942	0.941	0.941	0.940
ranolazine_mpo	0.821	0.818	0.809	0.820	0.819	0.804	0.760	0.728
scaffold_hop	0.628	0.621	0.617	0.576	0.615	0.527	0.560	0.517
sitagliptin_mpo	0.573	0.560	0.573	0.601	0.634	0.582	0.021	0.433
thiothixene_rediscovery	0.687	0.686	0.650	0.584	0.583	0.519	0.534	0.479
troglitazone_rediscovery	0.867	0.853	0.801	0.448	0.511	0.427	0.441	0.390
valsartan_smarts	0.797	0.797	0.739	0.627	0.135	0.000	0.178	0.000
zaleplon_mpo	0.569	0.569	0.406	0.486	0.552	0.519	0.358	0.346
Sum	18.208	18.091	17.641	16.928	16.213	14.708	14.196	13.751

remasking using GenMol. The fragment vocabulary is dynamically updated throughout the generation process, allowing exploration beyond the initial fragments. We adopt the practical molecular optimization (PMO) benchmark (Gao et al., 2022) which contains 23 optimization tasks. Following the benchmark setting, the maximum number of oracle calls is set to 10,000 and optimization performance is measured using the area under the curve (AUC) of the average top-10 property scores versus oracle calls. Further details are provided in Section A.5.

Baselines. As our baselines, we adopt the three recent state-of-the-art methods of the PMO benchmark. We also report performance of the top two methods reported by Gao et al. (2022). Note that as the paper of Gao et al. (2022) contains the results of a total of 25 methods, comparing GenMol to the top methods is equivalent to comparing it to 25 methods. The results of additional baselines including the standard deviations are provided in Table 5, Table 6, and Table 7. **Graph GA** (Jensen, 2019) is a GA that performs a random fragment-level crossover and a random atom- or bond-level mutation, and ***f*-RAG** (Lee et al., 2024a) is a method that uses fragment-level retrieval-augmented generation (RAG) and Graph GA-based fragment modification. **Genetic GFN** (Kim et al., 2024) utilizes Graph GA to guide a GFlowNet. **Mol GA** (Tripp & Hernández-Lobato, 2023) is a tuned version of Graph GA. **REIN-**

VENT (Olivecrona et al., 2017) is a reinforcement learning (RL) model based on the SMILES representation. We additionally compare GenMol with **GenMol-TR** and **GenMol-NR**, the ablated variants of GenMol which will be discussed in Section 5.5.

Results. The results of goal-directed hit generation are shown in Table 3. GenMol significantly outperforms the previous methods in terms of the sum AUC top-10 value and exhibits the best performance in 18 out of 23 tasks by a large margin. These results verify that the proposed optimization strategy of fragment remasking is effective in exploring chemical space and discovering optimized hit molecules. The results of GenMol trained on the ZINC250k dataset are shown in Table 8.

5.4. Goal-directed Lead Optimization

Setup. In goal-directed lead optimization, the goal is to generate leads when an initial seed molecule is given. Here, *leads* are defined as the molecules that exhibit improved target properties while maintaining the similarity with the given seed. We adopt the setting of Wang et al. (2023), where the objective is to optimize the binding affinity to the target protein while satisfying the following constraints: $\text{QED} \geq 0.6$, $\text{SA} \leq 4$, and $\text{sim} \geq \delta$ where $\delta \in \{0.4, 0.6\}$ and sim is the pairwise Tanimoto similarity between the Morgan fingerprints of the generated molecules and the

Table 4 | **Lead optimization results (kcal/mol).** The results are the docking scores of the most optimized leads. Lower is better, and the best results are highlighted in bold.

Target protein	Seed score	$\delta = 0.4$					$\delta = 0.6$				
		GenMol	GenMol-TR	GenMol-NR	RetMol	Graph GA	GenMol	GenMol-TR	GenMol-NR	RetMol	Graph GA
parp1	-7.3	-10.6	-8.7	-8.2	-9.0	-8.3	-10.4	-8.1	-8.3	-	-8.6
	-7.8	-11.0	-8.2	-8.3	-10.7	-8.9	-10.5	-8.2	-8.1	-	-8.1
	-8.2	-11.5	-10.9	-	-	-	-9.5	-8.7	-	-	-
fa7	-6.4	-7.5	-7.8	-7.2	-8.0	-7.8	-7.0	-	-	-7.6	-7.6
	-6.7	-8.4	-8.0	-8.3	-	-8.2	-7.6	-7.6	-	-	-7.6
	-8.5	-	-	-	-	-	-	-	-	-	-
5ht1b	-4.5	-12.9	-12.8	-	-12.1	-11.7	-12.1	-11.0	-	-	-11.3
	-7.6	-12.3	-11.8	-11.9	-9.0	-12.1	-12.2	-11.8	-12.6	-10.0	-12.0
	-9.8	-11.8	-11.3	-	-	-	-11.0	-10.7	-	-	-
braf	-9.3	-10.8	-10.7	-9.7	-	-9.8	-	-	-	-	-
	-9.4	-10.2	-10.8	-	-11.6	-	-10.2	-	-9.6	-	-
	-9.8	-10.6	-10.5	-	-	-11.6	-10.2	-10.0	-	-	-10.4
jak2	-7.7	-10.0	-8.7	-8.6	-8.2	-8.7	-9.5	-8.1	-8.0	-	-8.1
	-8.0	-9.9	-9.0	-8.9	-9.0	-9.2	-9.4	-9.0	-8.9	-	-9.2
	-8.6	-9.5	-9.2	-	-	-	-	-	-	-	-

seed. Optimization performance is evaluated by the docking score of the most optimized molecule that satisfies the above constraints. Following Lee et al. (2023), we adopt five target proteins, **parp1**, **fa7**, **5ht1b**, **braf**, and **jak2** to avoid bias in target selection. For each target, three molecules from its known active molecules are selected and each is given as a seed molecule, yielding a total of 15 tasks. As in Section 5.2, a fragment vocabulary is first constructed by fragmenting the seed molecule. A molecule is generated by randomly attaching two fragments from the vocabulary, and then applying GenMol’s fragment remasking. If the generated molecule is lead, its fragments are added to the fragment vocabulary. Further details are provided in Section A.6.

Baselines. Following Wang et al. (2023), we adopt **Graph GA** introduced in Section 5.3 and **Ret-Mol** (Wang et al., 2023), a retrieval-based molecular optimization method that uses retrieved molecules to guide the generation of a molecular language model, as our baselines. **GenMol-TR** and **GenMol-NR** are the ablated variants of GenMol which will be discussed in Section 5.5.

Results. The results of goal-directed lead optimization are shown in Table 4. As shown in the table, GenMol outperforms the baselines in most tasks. Note that baselines often fail, i.e., they cannot generate molecules with a higher binding affinity than the seed molecule while satisfying the constraints, especially under the harsher ($\delta = 0.6$) similarity constraint. In contrast, GenMol is able to successfully optimize most seed molecules, validating its effectiveness in exploring chemical space to optimize given molecules and discover promising lead molecules. The results of GenMol trained on the ZINC250k dataset (Irwin et al., 2012) are shown in Table 9.

5.5. Ablation Study

To examine the effect of the proposed fragment remasking scheme of GenMol, we compare GenMol with **GenMol-token remasking (GenMol-TR)**, GenMol that randomly masks individual tokens instead of masking a fragment chunk, and **GenMol-no remasking (GenMol-NR)**, GenMol that performs no remasking at all (i.e., relies solely on attaching random fragments of the fragment vocabulary to generate molecules), in Table 3 and Table 4. Both GenMol and GenMol-token remasking outperform GenMol-no remasking. Especially, GenMol-no remasking fails more frequently in the lead optimization task, highlighting the importance of the exploration strategy through remasking of masked diffusion models. On the other hand, GenMol outperforms GenMol-token remasking, proving that the proposed fragment remasking strategy is well aligned with chemical intuition and is therefore effective in exploring the chemical space to discover novel chemical optima.

6. Conclusion

We proposed GenMol, a versatile molecule generation framework designed to deal with various scenarios of drug discovery. By integrating discrete diffusion with the SAFE molecular representation, GenMol is able to effectively and efficiently generate molecules under settings that simulate a variety of drug discovery problems. Especially, the fragment remasking strategy that uses fragments as an explorative unit allows GenMol to effectively explore chemical space and discover chemical optima. Our experimental results showed that GenMol is capable of achieving state-of-the-art results in a wide range of drug discovery tasks, demonstrating the potential of GenMol as a unified and versatile tool for drug discovery.

References

Austin, J., Johnson, D. D., Ho, J., Tarlow, D., and Van Den Berg, R. Structured denoising diffusion models in discrete state-spaces. *Advances in Neural Information Processing Systems*, 34:17981–17993, 2021.

Bickerton, G. R., Paolini, G. V., Besnard, J., Muresan, S., and Hopkins, A. L. Quantifying the chemical beauty of drugs. *Nature chemistry*, 4(2):90–98, 2012.

Bohacek, R. S., McMardin, C., and Guida, W. C. The art and practice of structure-based drug design: a molecular modeling perspective. *Medicinal research reviews*, 16(1):3–50, 1996.

Campbell, A., Benton, J., De Bortoli, V., Rainforth, T., Deligiannidis, G., and Doucet, A. A continuous time framework for discrete denoising models. *Advances in Neural Information Processing Systems*, 35:28266–28279, 2022.

Chambers, J., Davies, M., Gaulton, A., Hersey, A., Velnkar, S., Petryszak, R., Hastings, J., Bellis, L., McGlinchey, S., and Overington, J. P. Unichem: a unified chemical structure cross-referencing and identifier tracking system. *Journal of cheminformatics*, 5(1):3, 2013.

Chang, H., Zhang, H., Jiang, L., Liu, C., and Freeman, W. T. Maskgit: Masked generative image transformer. In *Proceedings of the IEEE/CVF Conference on Computer Vision and Pattern Recognition*, pp. 11315–11325, 2022.

Degen, J., Wegscheid-Gerlach, C., Zaliani, A., and Rarey, M. On the art of compiling and using 'drug-like' chemical fragment spaces. *ChemMedChem: Chemistry Enabling Drug Discovery*, 3(10):1503–1507, 2008.

Devlin, J., Chang, M.-W., Lee, K., and Toutanova, K. Bert: Pre-training of deep bidirectional transformers for language understanding. In *Proceedings of naacl-HLT*, 2019.

Ertl, P. and Schuffenhauer, A. Estimation of synthetic accessibility score of drug-like molecules based on molecular complexity and fragment contributions. *Journal of cheminformatics*, 1:1–11, 2009.

Gao, W., Fu, T., Sun, J., and Coley, C. Sample efficiency matters: a benchmark for practical molecular optimization. *Advances in Neural Information Processing Systems*, 35:21342–21357, 2022.

Geng, Z., Xie, S., Xia, Y., Wu, L., Qin, T., Wang, J., Zhang, Y., Wu, F., and Liu, T.-Y. De novo molecular generation via connection-aware motif mining. In *International Conference on Learning Representations*, 2023.

Gruver, N., Stanton, S., Frey, N., Rudner, T. G., Hotzel, I., Lafrance-Vanasse, J., Rajpal, A., Cho, K., and Wilson, A. G. Protein design with guided discrete diffusion. *Advances in neural information processing systems*, 36, 2024.

Guo, J., Knuth, F., Margreitter, C., Janet, J. P., Papadopoulos, K., Engkvist, O., and Patronov, A. Linkinvent: generative linker design with reinforcement learning. *Digital Discovery*, 2(2):392–408, 2023.

Hayes, T., Rao, R., Akin, H., Sofroniew, N. J., Oktay, D., Lin, Z., Verkuil, R., Tran, V. Q., Deaton, J., Wiggert, M., et al. Simulating 500 million years of evolution with a language model. *bioRxiv*, pp. 2024–07, 2024.

He, Z., Sun, T., Tang, Q., Wang, K., Huang, X., and Qiu, X. Diffusionbert: Improving generative masked language models with diffusion models. In *The 61st Annual Meeting Of The Association For Computational Linguistics*, 2023.

Hoogeboom, E., Nielsen, D., Jaini, P., Forré, P., and Welling, M. Argmax flows and multinomial diffusion: Learning categorical distributions. *Advances in Neural Information Processing Systems*, 34:12454–12465, 2021.

Hua, C., Luan, S., Xu, M., Ying, Z., Fu, J., Ermon, S., and Precup, D. Mudiff: Unified diffusion for complete molecule generation. In *Learning on Graphs Conference*, pp. 33–1. PMLR, 2024.

Huang, K., Fu, T., Gao, W., Zhao, Y., Roohani, Y. H., Leskovec, J., Coley, C. W., Xiao, C., Sun, J., and Zitnik, M. Therapeutics data commons: Machine learning datasets and tasks for drug discovery and development. In *NeurIPS Track Datasets and Benchmarks*, 2021.

Hughes, J. P., Rees, S., Kalindjian, S. B., and Philpott, K. L. Principles of early drug discovery. *British journal of pharmacology*, 162(6):1239–1249, 2011.

Irwin, J. J. and Shoichet, B. K. Zinc- a free database of commercially available compounds for virtual screening. *Journal of chemical information and modeling*, 45(1):177–182, 2005.

Irwin, J. J., Sterling, T., Mysinger, M. M., Bolstad, E. S., and Coleman, R. G. Zinc: a free tool to discover chemistry for biology. *Journal of chemical information and modeling*, 52(7):1757–1768, 2012.

Jensen, J. H. A graph-based genetic algorithm and generative model/monte carlo tree search for the exploration of chemical space. *Chemical science*, 10(12):3567–3572, 2019.

Jin, W., Barzilay, R., and Jaakkola, T. Junction tree variational autoencoder for molecular graph generation. In *International Conference on Machine Learning*, pp. 2323–2332. PMLR, 2018.

Jin, W., Barzilay, R., and Jaakkola, T. Multi-objective molecule generation using interpretable substructures. In *International conference on machine learning*, pp. 4849–4859. PMLR, 2020.

Kim, H., Kim, M., Choi, S., and Park, J. Genetic-guided gflownets: Advancing in practical molecular optimization benchmark. *Advances in Neural Information Processing Systems*, 2024.

Kong, X., Huang, W., Tan, Z., and Liu, Y. Molecule generation by principal subgraph mining and assembling. *Advances in Neural Information Processing Systems*, 35:2550–2563, 2022.

Landrum, G. et al. RDKit: Open-source cheminformatics software, 2016. URL <http://www.rdkit.org/>, <https://github.com/rdkit/rdkit>, 2016.

Lee, S., Jo, J., and Hwang, S. J. Exploring chemical space with score-based out-of-distribution generation. In *International Conference on Machine Learning*, pp. 18872–18892. PMLR, 2023.

Lee, S., Kreis, K., Veccham, S. P., Liu, M., Reidenbach, D., Paliwal, S., Vahdat, A., and Nie, W. Molecule generation with fragment retrieval augmentation. *Advances in Neural Information Processing Systems*, 2024a.

Lee, S., Lee, S., Kawaguchi, K., and Hwang, S. J. Drug discovery with dynamic goal-aware fragments. *International Conference on Machine Learning*, 2024b.

Lin, H., Huang, Y., Zhang, O., Ma, S., Liu, M., Li, X., Wu, L., Ji, S., Hou, T., and Li, S. Z. Diffbp: Generative diffusion of 3d molecules for target protein binding. *Chemical Science*, 2024.

Loshchilov, I. and Hutter, F. Decoupled weight decay regularization. *International Conference on Learning Representations*, 2019.

Lou, A., Meng, C., and Ermon, S. Discrete diffusion language modeling by estimating the ratios of the data distribution. *International Conference on Machine Learning*, 2024.

Maziarz, K., Jackson-Flux, H. R., Cameron, P., Sirockin, F., Schneider, N., Stiefl, N., Segler, M., and Brockschmidt, M. Learning to extend molecular scaffolds with structural motifs. In *International Conference on Learning Representations*, 2021.

Murray, C. W. and Rees, D. C. The rise of fragment-based drug discovery. *Nature chemistry*, 1(3):187–192, 2009.

Noutahi, E., Gabellini, C., Craig, M., Lim, J. S., and Tossou, P. Gotta be safe: a new framework for molecular design. *Digital Discovery*, 3(4):796–804, 2024.

Olivcrona, M., Blaschke, T., Engkvist, O., and Chen, H. Molecular de-novo design through deep reinforcement learning. *Journal of cheminformatics*, 9(1):1–14, 2017.

Sahoo, S. S., Arriola, M., Schiff, Y., Gokaslan, A., Marroquin, E., Chiu, J. T., Rush, A., and Kuleshov, V. Simple and effective masked diffusion language models. *Advances in Neural Information Processing Systems*, 2024.

Shi, J., Han, K., Wang, Z., Doucet, A., and Titsias, M. K. Simplified and generalized masked diffusion for discrete data. *Advances in neural information processing systems*, 2024.

Sohl-Dickstein, J., Weiss, E., Maheswaranathan, N., and Ganguli, S. Deep unsupervised learning using nonequilibrium thermodynamics. In *International conference on machine learning*, pp. 2256–2265. PMLR, 2015.

Tang, Z., Gu, S., Bao, J., Chen, D., and Wen, F. Improved vector quantized diffusion models. *arXiv preprint arXiv:2205.16007*, 2022.

Tripp, A. and Hernández-Lobato, J. M. Genetic algorithms are strong baselines for molecule generation. *arXiv preprint arXiv:2310.09267*, 2023.

Vignac, C., Krawczuk, I., Sirauidin, A., Wang, B., Cevher, V., and Frossard, P. Digress: Discrete denoising diffusion for graph generation. In *Proceedings of the 11th International Conference on Learning Representations*, 2023.

Wang, Z., Nie, W., Qiao, Z., Xiao, C., Baraniuk, R., and Anandkumar, A. Retrieval-based controllable molecule generation. In *International Conference on Learning Representations*, 2023.

Weininger, D. Smiles, a chemical language and information system. 1. introduction to methodology and encoding rules. *Journal of chemical information and computer sciences*, 28(1):31–36, 1988.

Wolf, T., Debut, L., Sanh, V., Chaumond, J., Delangue, C., Moi, A., Cistac, P., Rault, T., Louf, R., Funtowicz, M., et al. Huggingface’s transformers: State-of-the-art natural language processing. arxiv. *arXiv preprint arXiv:1910.03771*, 2019.

Xie, Y., Shi, C., Zhou, H., Yang, Y., Zhang, W., Yu, Y., and Li, L. Mars: Markov molecular sampling for multi-objective drug discovery. In *International Conference on Learning Representations*, 2020.

Yang, S., Hwang, D., Lee, S., Ryu, S., and Hwang, S. J. Hit and lead discovery with explorative rl and fragment-based molecule generation. *Advances in Neural Information Processing Systems*, 34:7924–7936, 2021.

Yang, Y., Zheng, S., Su, S., Zhao, C., Xu, J., and Chen, H. Syntalinker: automatic fragment linking with deep conditional transformer neural networks. *Chemical science*, 11(31):8312–8322, 2020.

Zhang, W., Wang, X., Smith, J., Eaton, J., Rees, B., and Gu, Q. Diffmol: 3d structured molecule generation with discrete denoising diffusion probabilistic models. In *ICML 2023 Workshop on Structured Probabilistic Inference \& Generative Modeling*, 2023.

Zheng, L., Yuan, J., Yu, L., and Kong, L. A reparameterized discrete diffusion model for text generation. *Conference on Language Modeling*, 2024.

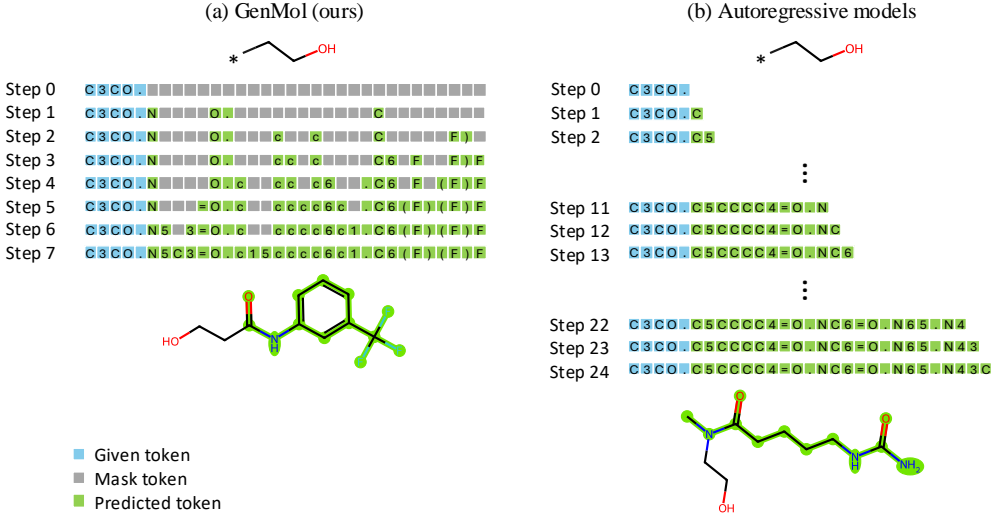


Figure 5 | **Illustration of the fragment-constrained motif extension process of (a) GenMol and (b) autoregressive models.** GenMol starts by sampling the length of the sequence and then filling the sequence with mask tokens corresponding to the sampled length. GenMol employs parallel decoding where all tokens are decoded simultaneously under discrete diffusion, and confirms only the most confident predictions. The decoding proceeds progressively until all mask tokens are predicted. In contrast, autoregressive models like SAFE-GPT (Noutahi et al., 2024) need to predict one token per step, requiring many more decoding steps.

A. Experimental Details

A.1. Computing Resources

GenMol was trained using 8 NVIDIA A100 GPUs. The training took approximately 6 hours. All the molecular generation experiments were conducted using a single NVIDIA A100 GPU and 32 CPU cores.

A.2. Training GenMol

In this section, we describe the details for training GenMol. We used the BERT (Devlin et al., 2019) architecture of the HuggingFace Transformers library (Wolf et al., 2019) with the default configuration, except that we set max_position_embeddings to 256. We used the SAFE dataset and SAFE tokenizer (Noutahi et al., 2024) that has a vocabulary size of $K = 1880$. We set the batch size to 2048, the learning rate to $3e-4$, and the number of training steps to 50k. We used the log-linear noise schedule of Sahoo et al. (2024) and the AdamW optimizer (Loshchilov & Hutter, 2019) with $\beta_1 = 0.9$ and $\beta_2 = 0.999$.

A.3. De Novo Generation

In this section, we describe the details for conducting experiments in Section 5.1. We used the RDKit library (Landrum et al., 2016) to obtain Morgan fingerprints and the Therapeutics Data Commons (TDC) library (Huang et al., 2021) to calculate diversity, QED, and SA. The lengths of the mask chunks were sampled from the ZINC250k distribution.

A.4. Fragment-constrained Generation

In Section 5.2, we used the benchmark proposed by Noutahi et al. (2024). The benchmark contains extracted fragments from 10 known drugs: Cyclothiazide, Maribavir, Spirapril, Baricitinib, Eliglustat, Erlotinib, Futibatinib, Lesinurad, Liothyronine, and Lovastatin. Specifically, from each drug, side chains, a starting motif, the main scaffold with attachment points, and a core substructure are extracted, and then serve as input for linker design & scaffold morphing, motif extension, scaffold decoration, and superstructure generation, respectively. **Linker design** and **scaffold morphing** are tasks where the goal is to generate a linker fragment that connects given two side chains. In GenMol, linker design and scaffold morphing correspond to the same

task. **Motif extension** and **scaffold decoration** are tasks where the goal is to generate a side fragment to complete a new molecule when a motif or scaffold and attachment points are given. **Superstructure generation** is a task where the goal is to generate a molecule when a substructure constraint is given. Following [Noutahi et al. \(2024\)](#), we first generate random attachment points on the substructure to create new scaffolds and conduct the scaffold decoration task.

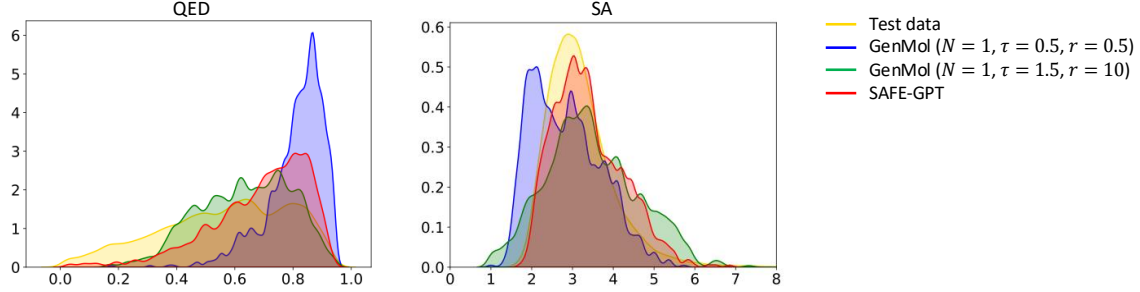
We used $N = 1$. We performed the grid search with the search space $\tau \in \{0.5, 0.8, 1, 1.2, 1.5\}$ and $r \in \{1, 1.2, 2, 3\}$, and set r to 3 for linker design and scaffold morphing, 1.2 for motif extension, and 2 for scaffold decoration and superstructure generation. We set τ to 1.2 for all the tasks. The lengths of the mask chunks were sampled from the ZINC250k distribution.

A.5. Goal-directed Hit Generation

In this section, we describe the details for conducting experiments in Section 5.3. To construct an initial fragment vocabulary, we adopted a simple decomposition rule that randomly cut one of the non-ring single bonds of a given molecules three times and apply it to the ZINC250k dataset. We set the size of the fragment vocabulary to 100. We applied the warmup scheme that let GenMol generate molecules by concatenating two randomly chosen fragments without fragment remasking for the first 1,000 generations. We used $N = 1$, $\tau = 1.2$, and $r = 2$.

A.6. Goal-directed Lead Optimization

In this section, we describe the details for conducting experiments in Section 5.4. Following the setting of [Wang et al. \(2023\)](#), for each target protein and each seed molecule, we run 10 optimization iterations with 100 generation per iteration. We adopted the same decomposition rule described in Section A.5 and used $N = 1$, $\tau = 1.2$, and $r = 2$.

Figure 6 | QED and SA distributions of molecules in *de novo* generation.

B. Additional Experimental Results

B.1. QED and SA Distributions in *De Novo* Generation

We provide the QED and SA distributions of molecules generated by GenMol and SAFE-GPT, respectively, in Figure 6. The distributions of 100k molecules randomly sampled from the test set are also shown in the figure. As shown in the figure, GenMol is able to generate molecules of higher QED (more drug-like) and lower SA (more synthesizable) values than SAFE-GPT, resulting in high quality in Table 1. Furthermore, GenMol can freely control these distributions by adjusting the values of the softmax temperature τ and the randomness r .

B.2. Analysis on Quality and Diversity in *De Novo* Generation

The quality and diversity values of 100k molecules randomly sampled from the test set are 38.2% and 0.897, respectively. The quality and diversity values of molecules generated by GenMol ($N = 1, \tau = 0.5, r = 0.5$) are 84.6% and 0.818, respectively, as shown in Table 1. We can think of this as sacrificing diversity and selecting a specific mode of high quality. GenMol can control this mode-selecting behavior by adjusting τ and r (e.g., the quality and diversity values of GenMol ($N = 1, \tau = 1.5, r = 10$) shown in Table 1 are 39.7% and 0.911, respectively).

B.3. Full Goal-directed Hit Generation Results

We provide the full results of Table 3 including the additional baselines from Gao et al. (2022) and the standard deviations in Table 5, Table 6, and Table 7. As shown in the tables, GenMol outperforms all the 28 baselines by a large margin.

B.4. Goal-directed Hit Generation Results of GenMol Variants

We provide the full results of the internal baselines in Table 3, GenMol-TR and GenMol-NR, and GenMol trained on the ZINC250k dataset (Irwin et al., 2012) instead of the SAFE dataset, GenMol-ZINC250k, in Table 8. As shown in the table, GenMol-ZINC250k shows comparable results to GenMol, while GenMol-TR and GenMol-NR show inferior performance to GenMol as discussed in Section 5.5.

B.5. Goal-directed Lead Optimization Results with ZINC250k

We provide the goal-directed lead optimization results of GenMol-ZINC250k in Table 9. As shown in the table, GenMol-ZINC250k shows comparable performance to GenMol, both showing superior performance to the baselines in Table 4.

Table 5 | **Goal-directed hit generation results.** The results are the means and standard deviations of PMO AUC top-10 of 3 runs. The results for *f*-RAG (Lee et al., 2024a), Genetic GFN (Kim et al., 2024) and Mol GA (Tripp & Hernández-Lobato, 2023) are taken from the respective papers and the results for other baselines are taken from Gao et al. (2022). The best results are highlighted in bold.

Oracle	GenMol	<i>f</i> -RAG	Genetic GFN	Mol GA	
albuterol_similarity	0.932 ± 0.007	0.977 ± 0.002	0.949 ± 0.010	0.896 ± 0.035	
amlodipine_mpo	0.804 ± 0.006	0.749 ± 0.019	0.761 ± 0.019	0.688 ± 0.039	
celecoxib_rediscovery	0.826 ± 0.018	0.778 ± 0.007	0.802 ± 0.029	0.567 ± 0.083	
deco_hop	0.953 ± 0.016	0.936 ± 0.011	0.733 ± 0.109	0.649 ± 0.025	
drd2	0.995 ± 0.000	0.992 ± 0.000	0.974 ± 0.006	0.936 ± 0.016	
fexofenadine_mpo	0.894 ± 0.028	0.856 ± 0.016	0.856 ± 0.039	0.825 ± 0.019	
gsk3b	0.986 ± 0.003	0.969 ± 0.003	0.881 ± 0.042	0.843 ± 0.039	
isomers_c7h8n2o2	0.934 ± 0.002	0.955 ± 0.008	0.969 ± 0.003	0.878 ± 0.026	
isomers_c9h10n2o2pf2cl	0.833 ± 0.014	0.850 ± 0.005	0.897 ± 0.007	0.865 ± 0.012	
jnk3	0.856 ± 0.016	0.904 ± 0.004	0.764 ± 0.069	0.702 ± 0.123	
median1	0.397 ± 0.000	0.340 ± 0.007	0.379 ± 0.010	0.257 ± 0.009	
median2	0.355 ± 0.003	0.323 ± 0.005	0.294 ± 0.007	0.301 ± 0.021	
mestranol_similarity	0.981 ± 0.003	0.671 ± 0.021	0.708 ± 0.057	0.591 ± 0.053	
osimertinib_mpo	0.876 ± 0.008	0.866 ± 0.009	0.860 ± 0.008	0.844 ± 0.015	
perindopril_mpo	0.703 ± 0.009	0.681 ± 0.017	0.595 ± 0.014	0.547 ± 0.022	
qed	0.942 ± 0.000	0.939 ± 0.001	0.942 ± 0.000	0.941 ± 0.001	
ranolazine_mpo	0.821 ± 0.011	0.820 ± 0.016	0.819 ± 0.018	0.804 ± 0.011	
scaffold_hop	0.628 ± 0.008	0.576 ± 0.014	0.615 ± 0.100	0.527 ± 0.025	
sitagliptin_mpo	0.573 ± 0.050	0.601 ± 0.011	0.634 ± 0.039	0.582 ± 0.040	
thiothixene_rediscovery	0.687 ± 0.125	0.584 ± 0.009	0.583 ± 0.034	0.519 ± 0.041	
troglitazone_rediscovery	0.867 ± 0.022	0.448 ± 0.017	0.511 ± 0.054	0.427 ± 0.031	
valsartan_smarts	0.797 ± 0.033	0.627 ± 0.058	0.135 ± 0.271	0.000 ± 0.000	
zaleplon_mpo	0.569 ± 0.005	0.486 ± 0.004	0.552 ± 0.033	0.519 ± 0.029	
Sum	18.208	16.928	16.213	14.708	
Oracle	REINVENT	Graph GA	SELFIES-REINVENT	GP BO	STONED
albuterol_similarity	0.882 ± 0.006	0.838 ± 0.016	0.826 ± 0.030	0.898 ± 0.014	0.745 ± 0.076
amlodipine_mpo	0.635 ± 0.035	0.661 ± 0.020	0.607 ± 0.014	0.583 ± 0.044	0.608 ± 0.046
celecoxib_rediscovery	0.713 ± 0.067	0.630 ± 0.097	0.573 ± 0.043	0.723 ± 0.053	0.382 ± 0.041
deco_hop	0.666 ± 0.044	0.619 ± 0.004	0.631 ± 0.012	0.629 ± 0.018	0.611 ± 0.008
drd2	0.945 ± 0.007	0.964 ± 0.012	0.943 ± 0.005	0.923 ± 0.017	0.913 ± 0.020
fexofenadine_mpo	0.784 ± 0.006	0.760 ± 0.011	0.741 ± 0.002	0.722 ± 0.005	0.797 ± 0.016
gsk3b	0.865 ± 0.043	0.788 ± 0.070	0.780 ± 0.037	0.851 ± 0.041	0.668 ± 0.049
isomers_c7h8n2o2	0.852 ± 0.036	0.862 ± 0.065	0.849 ± 0.034	0.680 ± 0.117	0.899 ± 0.011
isomers_c9h10n2o2pf2cl	0.642 ± 0.054	0.719 ± 0.047	0.733 ± 0.029	0.469 ± 0.180	0.805 ± 0.031
jnk3	0.783 ± 0.023	0.553 ± 0.136	0.631 ± 0.064	0.564 ± 0.155	0.523 ± 0.092
median1	0.356 ± 0.009	0.294 ± 0.021	0.355 ± 0.011	0.301 ± 0.014	0.266 ± 0.016
median2	0.276 ± 0.008	0.273 ± 0.009	0.255 ± 0.005	0.297 ± 0.009	0.245 ± 0.032
mestranol_similarity	0.618 ± 0.048	0.579 ± 0.022	0.620 ± 0.029	0.627 ± 0.089	0.609 ± 0.101
osimertinib_mpo	0.837 ± 0.009	0.831 ± 0.005	0.820 ± 0.003	0.787 ± 0.006	0.822 ± 0.012
perindopril_mpo	0.537 ± 0.016	0.538 ± 0.009	0.517 ± 0.021	0.493 ± 0.011	0.488 ± 0.011
qed	0.941 ± 0.000	0.940 ± 0.000	0.940 ± 0.000	0.937 ± 0.000	0.941 ± 0.000
ranolazine_mpo	0.760 ± 0.009	0.728 ± 0.012	0.748 ± 0.018	0.735 ± 0.013	0.765 ± 0.029
scaffold_hop	0.560 ± 0.019	0.517 ± 0.007	0.525 ± 0.013	0.548 ± 0.019	0.521 ± 0.034
sitagliptin_mpo	0.021 ± 0.003	0.433 ± 0.075	0.194 ± 0.121	0.186 ± 0.055	0.393 ± 0.083
thiothixene_rediscovery	0.534 ± 0.013	0.479 ± 0.025	0.495 ± 0.040	0.559 ± 0.027	0.367 ± 0.027
troglitazone_rediscovery	0.441 ± 0.032	0.390 ± 0.016	0.348 ± 0.012	0.410 ± 0.015	0.320 ± 0.018
valsartan_smarts	0.179 ± 0.358	0.000 ± 0.000	0.000 ± 0.000	0.000 ± 0.000	0.000 ± 0.000
zaleplon_mpo	0.358 ± 0.062	0.346 ± 0.032	0.333 ± 0.026	0.221 ± 0.072	0.325 ± 0.027
Sum	14.196	13.751	13.471	13.156	13.024

Table 6 | Goal-directed hit generation results (continued).

Oracle	LSTM HC	SMILES-GA	SynNet	DoG-Gen	DST
albuterol_similarity	0.719 ± 0.018	0.661 ± 0.066	0.584 ± 0.039	0.676 ± 0.013	0.619 ± 0.020
amlodipine_mpo	0.593 ± 0.016	0.549 ± 0.009	0.565 ± 0.007	0.536 ± 0.003	0.516 ± 0.007
celecoxib_rediscovery	0.539 ± 0.018	0.344 ± 0.027	0.441 ± 0.027	0.464 ± 0.009	0.380 ± 0.006
deco_hop	0.826 ± 0.017	0.611 ± 0.006	0.613 ± 0.009	0.800 ± 0.007	0.608 ± 0.008
drd2	0.919 ± 0.015	0.908 ± 0.019	0.969 ± 0.004	0.948 ± 0.001	0.820 ± 0.014
fexofenadine_mpo	0.725 ± 0.003	0.721 ± 0.015	0.761 ± 0.015	0.695 ± 0.003	0.725 ± 0.005
gsk3b	0.839 ± 0.015	0.629 ± 0.044	0.789 ± 0.032	0.831 ± 0.021	0.671 ± 0.032
isomers_c7h8n2o2	0.485 ± 0.045	0.913 ± 0.021	0.455 ± 0.031	0.465 ± 0.018	0.548 ± 0.069
isomers_c9h10n2o2pf2cl	0.342 ± 0.027	0.860 ± 0.065	0.241 ± 0.064	0.199 ± 0.016	0.458 ± 0.063
jnk3	0.661 ± 0.039	0.316 ± 0.022	0.630 ± 0.034	0.595 ± 0.023	0.556 ± 0.057
median1	0.255 ± 0.010	0.192 ± 0.012	0.218 ± 0.008	0.217 ± 0.001	0.232 ± 0.009
median2	0.248 ± 0.008	0.198 ± 0.005	0.235 ± 0.006	0.212 ± 0.000	0.185 ± 0.020
mestranol_similarity	0.526 ± 0.032	0.469 ± 0.029	0.399 ± 0.021	0.437 ± 0.007	0.450 ± 0.027
osimertinib_mpo	0.796 ± 0.002	0.817 ± 0.011	0.796 ± 0.003	0.774 ± 0.002	0.785 ± 0.004
perindopril_mpo	0.489 ± 0.007	0.447 ± 0.013	0.557 ± 0.011	0.474 ± 0.002	0.462 ± 0.008
qed	0.939 ± 0.000	0.940 ± 0.000	0.941 ± 0.000	0.934 ± 0.000	0.938 ± 0.000
ranolazine_mpo	0.714 ± 0.008	0.699 ± 0.026	0.741 ± 0.010	0.711 ± 0.006	0.632 ± 0.054
scaffold_hop	0.533 ± 0.012	0.494 ± 0.011	0.502 ± 0.012	0.515 ± 0.005	0.497 ± 0.004
sitagliptin_mpo	0.066 ± 0.019	0.363 ± 0.057	0.025 ± 0.014	0.048 ± 0.008	0.075 ± 0.032
thiothixene_rediscovery	0.438 ± 0.008	0.315 ± 0.017	0.401 ± 0.019	0.375 ± 0.004	0.366 ± 0.006
troglitazone_rediscovery	0.354 ± 0.016	0.263 ± 0.024	0.283 ± 0.008	0.416 ± 0.019	0.279 ± 0.019
valsartan_smarts	0.000 ± 0.000	0.000 ± 0.000	0.000 ± 0.000	0.000 ± 0.000	0.000 ± 0.000
zaleplon_mpo	0.206 ± 0.006	0.334 ± 0.041	0.341 ± 0.011	0.123 ± 0.016	0.176 ± 0.045
Sum	12.223	12.054	11.498	11.456	10.989

Oracle	MARS	MIMOSA	MolPal	SELFIES-LSTM HC	DoG-AE
albuterol_similarity	0.597 ± 0.124	0.618 ± 0.017	0.609 ± 0.002	0.664 ± 0.030	0.533 ± 0.034
amlodipine_mpo	0.504 ± 0.016	0.543 ± 0.003	0.582 ± 0.008	0.532 ± 0.004	0.507 ± 0.005
celecoxib_rediscovery	0.379 ± 0.060	0.393 ± 0.010	0.415 ± 0.001	0.385 ± 0.008	0.355 ± 0.012
deco_hop	0.589 ± 0.003	0.619 ± 0.003	0.643 ± 0.005	0.590 ± 0.001	0.765 ± 0.055
drd2	0.891 ± 0.020	0.799 ± 0.017	0.783 ± 0.009	0.729 ± 0.034	0.943 ± 0.009
fexofenadine_mpo	0.711 ± 0.006	0.706 ± 0.011	0.685 ± 0.000	0.693 ± 0.004	0.679 ± 0.017
gsk3b	0.552 ± 0.037	0.554 ± 0.042	0.555 ± 0.011	0.423 ± 0.018	0.601 ± 0.091
isomers_c7h8n2o2	0.728 ± 0.027	0.564 ± 0.046	0.484 ± 0.006	0.587 ± 0.031	0.239 ± 0.077
isomers_c9h10n2o2pf2cl	0.581 ± 0.013	0.303 ± 0.046	0.164 ± 0.003	0.352 ± 0.019	0.049 ± 0.015
jnk3	0.489 ± 0.095	0.360 ± 0.063	0.339 ± 0.009	0.207 ± 0.013	0.469 ± 0.138
median1	0.207 ± 0.011	0.243 ± 0.005	0.249 ± 0.001	0.239 ± 0.009	0.171 ± 0.009
median2	0.181 ± 0.011	0.214 ± 0.002	0.230 ± 0.000	0.205 ± 0.005	0.182 ± 0.006
mestranol_similarity	0.388 ± 0.026	0.438 ± 0.015	0.564 ± 0.004	0.446 ± 0.009	0.370 ± 0.014
osimertinib_mpo	0.777 ± 0.006	0.788 ± 0.014	0.779 ± 0.000	0.780 ± 0.005	0.750 ± 0.012
perindopril_mpo	0.462 ± 0.006	0.490 ± 0.011	0.467 ± 0.002	0.448 ± 0.006	0.432 ± 0.013
qed	0.930 ± 0.003	0.939 ± 0.000	0.940 ± 0.000	0.938 ± 0.000	0.926 ± 0.003
ranolazine_mpo	0.740 ± 0.010	0.640 ± 0.015	0.457 ± 0.005	0.614 ± 0.010	0.689 ± 0.015
scaffold_hop	0.469 ± 0.004	0.507 ± 0.015	0.494 ± 0.000	0.472 ± 0.002	0.489 ± 0.010
sitagliptin_mpo	0.016 ± 0.003	0.102 ± 0.023	0.043 ± 0.001	0.116 ± 0.012	0.009 ± 0.005
thiothixene_rediscovery	0.344 ± 0.022	0.347 ± 0.018	0.339 ± 0.001	0.339 ± 0.009	0.314 ± 0.015
troglitazone_rediscovery	0.256 ± 0.016	0.299 ± 0.009	0.268 ± 0.000	0.257 ± 0.002	0.259 ± 0.016
valsartan_smarts	0.000 ± 0.000	0.000 ± 0.000	0.000 ± 0.000	0.000 ± 0.000	0.000 ± 0.000
zaleplon_mpo	0.187 ± 0.046	0.172 ± 0.036	0.168 ± 0.003	0.218 ± 0.020	0.049 ± 0.027
Sum	10.989	10.651	10.268	10.246	9.790

Table 7 | Goal-directed hit generation results (continued).

Oracle	GFlowNet	GA+D	SELFIES-VAE BO	Screening	SMILES-VAE BO
albuterol_similarity	0.447 ± 0.012	0.495 ± 0.025	0.494 ± 0.012	0.483 ± 0.006	0.489 ± 0.007
amlodipine_mpo	0.444 ± 0.004	0.400 ± 0.032	0.516 ± 0.005	0.535 ± 0.001	0.533 ± 0.009
celecoxib_rediscovery	0.327 ± 0.004	0.223 ± 0.025	0.326 ± 0.007	0.351 ± 0.005	0.354 ± 0.002
deco_hop	0.583 ± 0.002	0.550 ± 0.005	0.579 ± 0.001	0.590 ± 0.001	0.589 ± 0.001
drd2	0.590 ± 0.070	0.382 ± 0.205	0.569 ± 0.039	0.545 ± 0.015	0.555 ± 0.043
fexofenadine_mpo	0.693 ± 0.006	0.587 ± 0.007	0.670 ± 0.004	0.666 ± 0.004	0.671 ± 0.003
gsk3b	0.651 ± 0.026	0.342 ± 0.019	0.350 ± 0.034	0.438 ± 0.034	0.386 ± 0.006
isomers_c7h8n2o2	0.366 ± 0.043	0.854 ± 0.015	0.325 ± 0.028	0.168 ± 0.034	0.161 ± 0.017
isomers_c9h10n2o2pf2cl	0.110 ± 0.031	0.657 ± 0.020	0.200 ± 0.030	0.106 ± 0.021	0.084 ± 0.009
jnk3	0.440 ± 0.022	0.219 ± 0.021	0.208 ± 0.022	0.238 ± 0.024	0.241 ± 0.026
median1	0.202 ± 0.004	0.180 ± 0.009	0.201 ± 0.003	0.205 ± 0.005	0.202 ± 0.006
median2	0.180 ± 0.000	0.121 ± 0.005	0.185 ± 0.001	0.200 ± 0.004	0.195 ± 0.001
mestranol_similarity	0.322 ± 0.007	0.371 ± 0.016	0.386 ± 0.009	0.409 ± 0.019	0.399 ± 0.005
osimertinib_mpo	0.784 ± 0.001	0.672 ± 0.027	0.765 ± 0.002	0.764 ± 0.001	0.771 ± 0.002
perindopril_mpo	0.430 ± 0.010	0.172 ± 0.088	0.429 ± 0.003	0.445 ± 0.004	0.442 ± 0.004
qed	0.921 ± 0.004	0.860 ± 0.014	0.936 ± 0.001	0.938 ± 0.000	0.938 ± 0.000
ranolazine_mpo	0.652 ± 0.002	0.555 ± 0.015	0.452 ± 0.025	0.411 ± 0.010	0.457 ± 0.012
scaffold_hop	0.463 ± 0.002	0.413 ± 0.009	0.455 ± 0.004	0.471 ± 0.002	0.470 ± 0.003
sitagliptin_mpo	0.008 ± 0.003	0.281 ± 0.022	0.084 ± 0.015	0.022 ± 0.003	0.023 ± 0.004
thiothixene_rediscovery	0.285 ± 0.012	0.223 ± 0.029	0.297 ± 0.004	0.317 ± 0.003	0.317 ± 0.007
troglitazone_rediscovery	0.188 ± 0.001	0.152 ± 0.013	0.243 ± 0.004	0.249 ± 0.003	0.257 ± 0.003
valsartan_smarts	0.000 ± 0.000	0.000 ± 0.000	0.002 ± 0.003	0.000 ± 0.000	0.002 ± 0.004
zaleplon_mpo	0.035 ± 0.030	0.244 ± 0.015	0.206 ± 0.015	0.072 ± 0.014	0.039 ± 0.012
Sum	9.131	8.964	8.887	8.635	8.587

Oracle	Pasithea	GFlowNet-AL	JT-VAE BO	Graph MCTS	MolDQN
albuterol_similarity	0.447 ± 0.007	0.390 ± 0.008	0.485 ± 0.029	0.580 ± 0.023	0.320 ± 0.015
amlodipine_mpo	0.504 ± 0.003	0.428 ± 0.002	0.519 ± 0.009	0.447 ± 0.008	0.311 ± 0.008
celecoxib_rediscovery	0.312 ± 0.007	0.257 ± 0.003	0.299 ± 0.009	0.264 ± 0.013	0.099 ± 0.005
deco_hop	0.579 ± 0.001	0.583 ± 0.001	0.585 ± 0.002	0.554 ± 0.002	0.546 ± 0.001
drd2	0.255 ± 0.040	0.468 ± 0.046	0.506 ± 0.136	0.300 ± 0.050	0.025 ± 0.001
fexofenadine_mpo	0.660 ± 0.015	0.688 ± 0.002	0.667 ± 0.010	0.574 ± 0.009	0.478 ± 0.012
gsk3b	0.281 ± 0.038	0.588 ± 0.015	0.350 ± 0.051	0.281 ± 0.022	0.241 ± 0.008
isomers_c7h8n2o2	0.673 ± 0.030	0.241 ± 0.055	0.103 ± 0.016	0.530 ± 0.035	0.431 ± 0.035
isomers_c9h10n2o2pf2cl	0.345 ± 0.145	0.064 ± 0.012	0.090 ± 0.035	0.454 ± 0.067	0.342 ± 0.026
jnk3	0.154 ± 0.018	0.362 ± 0.021	0.222 ± 0.009	0.110 ± 0.019	0.111 ± 0.008
median1	0.178 ± 0.009	0.190 ± 0.002	0.179 ± 0.003	0.195 ± 0.005	0.122 ± 0.007
median2	0.179 ± 0.004	0.173 ± 0.001	0.180 ± 0.003	0.132 ± 0.002	0.088 ± 0.003
mestranol_similarity	0.361 ± 0.016	0.295 ± 0.004	0.356 ± 0.013	0.281 ± 0.008	0.188 ± 0.007
osimertinib_mpo	0.749 ± 0.007	0.787 ± 0.003	0.775 ± 0.004	0.700 ± 0.004	0.674 ± 0.006
perindopril_mpo	0.421 ± 0.008	0.421 ± 0.002	0.430 ± 0.009	0.277 ± 0.013	0.213 ± 0.043
qed	0.931 ± 0.002	0.902 ± 0.005	0.934 ± 0.002	0.892 ± 0.006	0.731 ± 0.018
ranolazine_mpo	0.347 ± 0.012	0.632 ± 0.007	0.508 ± 0.055	0.239 ± 0.027	0.051 ± 0.020
scaffold_hop	0.456 ± 0.003	0.460 ± 0.002	0.470 ± 0.005	0.412 ± 0.003	0.405 ± 0.004
sitagliptin_mpo	0.088 ± 0.013	0.006 ± 0.001	0.046 ± 0.027	0.056 ± 0.012	0.003 ± 0.002
thiothixene_rediscovery	0.288 ± 0.006	0.266 ± 0.005	0.282 ± 0.008	0.231 ± 0.004	0.099 ± 0.007
troglitazone_rediscovery	0.240 ± 0.002	0.186 ± 0.003	0.237 ± 0.005	0.224 ± 0.009	0.122 ± 0.004
valsartan_smarts	0.006 ± 0.012	0.000 ± 0.000	0.000 ± 0.000	0.000 ± 0.000	0.000 ± 0.000
zaleplon_mpo	0.091 ± 0.013	0.010 ± 0.001	0.125 ± 0.038	0.058 ± 0.019	0.010 ± 0.005
Sum	8.556	8.406	8.358	7.803	5.620

Table 8 | **Goal-directed hit generation results** of GenMol variants. The results are the means and standard deviations of PMO AUC top-10 of 3 runs. The best results are highlighted in bold.

Oracle	GenMol	GenMol-ZINC250k	GenMol-TR	GenMol-NR
albuterol_similarity	0.932 ± 0.007	0.912 ± 0.008	0.895 ± 0.033	0.872 ± 0.032
amlodipine_mpo	0.804 ± 0.006	0.797 ± 0.031	0.802 ± 0.016	0.769 ± 0.029
celecoxib_rediscovery	0.826 ± 0.018	0.826 ± 0.012	0.821 ± 0.010	0.859 ± 0.008
deco_hop	0.953 ± 0.016	0.954 ± 0.019	0.945 ± 0.006	0.917 ± 0.009
drd2	0.995 ± 0.000	0.995 ± 0.000	0.995 ± 0.000	0.995 ± 0.000
fexofenadine_mpo	0.894 ± 0.028	0.893 ± 0.028	0.886 ± 0.017	0.875 ± 0.019
gsk3b	0.986 ± 0.003	0.988 ± 0.003	0.985 ± 0.003	0.985 ± 0.003
isomers_c7h8n2o2	0.934 ± 0.002	0.938 ± 0.003	0.934 ± 0.003	0.897 ± 0.016
isomers_c9h10n2o2pf2cl	0.833 ± 0.014	0.838 ± 0.014	0.830 ± 0.016	0.816 ± 0.025
jnk3	0.856 ± 0.016	0.856 ± 0.019	0.848 ± 0.016	0.845 ± 0.035
median1	0.397 ± 0.000	0.398 ± 0.001	0.397 ± 0.000	0.397 ± 0.000
median2	0.355 ± 0.003	0.352 ± 0.008	0.350 ± 0.006	0.349 ± 0.004
mestranol_similarity	0.981 ± 0.003	0.981 ± 0.003	0.980 ± 0.002	0.970 ± 0.004
osimertinib_mpo	0.876 ± 0.008	0.880 ± 0.000	0.876 ± 0.008	0.876 ± 0.003
perindopril_mpo	0.703 ± 0.009	0.708 ± 0.004	0.703 ± 0.006	0.697 ± 0.014
qed	0.942 ± 0.000	0.942 ± 0.000	0.942 ± 0.000	0.927 ± 0.000
ranolazine_mpo	0.821 ± 0.011	0.821 ± 0.023	0.818 ± 0.016	0.809 ± 0.009
scaffold_hop	0.628 ± 0.008	0.632 ± 0.001	0.621 ± 0.012	0.617 ± 0.002
sitagliptin_mpo	0.573 ± 0.050	0.596 ± 0.003	0.560 ± 0.037	0.573 ± 0.006
thiothixene_rediscovery	0.687 ± 0.125	0.686 ± 0.103	0.686 ± 0.121	0.650 ± 0.073
troglitazone_rediscovery	0.867 ± 0.022	0.827 ± 0.062	0.853 ± 0.035	0.801 ± 0.062
valsartan_smarts	0.797 ± 0.033	0.797 ± 0.036	0.797 ± 0.036	0.739 ± 0.043
zaleplon_mpo	0.569 ± 0.005	0.597 ± 0.008	0.569 ± 0.014	0.406 ± 0.002
Sum	18.208	18.207	18.091	17.641

Table 9 | **Lead optimization results (kcal/mol)** of GenMol variants. The results are the docking scores of the most optimized leads. Lower is better, and the best results are highlighted in bold.

Target protein	Seed score	$\delta = 0.4$		$\delta = 0.6$	
		GenMol	GenMol-ZINC250k	GenMol	GenMol-ZINC250k
parp1	-7.3	-10.6	-10.5	-10.4	-10.6
	-7.8	-11.0	-11.2	-10.5	-10.5
	-8.2	-11.5	-10.1	-9.5	-8.8
fa7	-6.4	-7.5	-7.9	-7.0	-
	-6.7	-8.4	-8.2	-7.6	-7.2
	-8.5	-	-	-	-
5ht1b	-4.5	-12.9	-12.9	-12.1	-12.0
	-7.6	-12.3	-12.0	-12.2	-11.8
	-9.8	-11.8	-10.5	-11.0	-11.0
braf	-9.3	-10.8	-10.7	-	-
	-9.4	-10.2	-11.5	-10.2	-10.0
	-9.8	-10.6	-10.6	-10.2	-10.0
jak2	-7.7	-10.0	-10.0	-9.5	-9.7
	-8.0	-9.9	-10.0	-9.4	-9.2
	-8.6	-9.5	-9.5	-	-